Published in final edited form as:
Biochem Pharmacol. 2009 August 15; 78(4): 355–364. doi:10.1016/j.bcp.2009.04.023.

Sensitization of ABCB1 Overexpressing Cells to Chemotherapeutic Agents by FG020326 via Binding to ABCB1 and Inhibiting Its Function

Chun-ling Dai[a], **Yong-ju Liang**[a], **Li-ming Chen**[a], **Xu Zhang**[a], **Wen-jing Deng**[a], **Xiao-dong Su**[a], **Zhi Shi**[a,b], **Chung-pu Wu**[c], **Charles R. Ashby Jr.**[b], **Shin-ichi Akiyama**[d], **Suresh V. Ambudkar**[c], **Zhe-sheng Chen**[b,*], and **Li-wu Fu**[a,*]

[a]State Key Laboratory of Oncology in South China, Cancer Center, Sun Yat-Sen University, Guangzhou 510060, China

[b]Department of Pharmaceutical Sciences, College of Pharmacy and Allied Health Professions, St John's University, Jamaica, NY 11439, USA

[c]Laboratory of Cell Biology, Center for Cancer Research, NCI, NIH, Bethesda, MD 20892, USA

[d]Department of Molecular Oncology, Kagoshima University Graduate School of Medicine and Dental Sciences, Kagoshima 890-8544, Japan

Abstract

The effectiveness of chemotherapeutic treatment is usually limited by the overexpression of adenosine triphosphate binding cassette (ABC) transporters, which mediate multidrug resistance (MDR) by acting as efflux pumps to remove chemotherapeutic agents from MDR cancer cells. Thus, the inhibition of ABC transporters may represent a promising strategy to reverse MDR. This study was to characterize the *in vitro* and *in vivo* actions of FG020326, a newly synthesized triaryl-substituted imidazole derivative, to reverse MDR. FG020326 significantly potentiated the cytotoxicity of paclitaxel, doxorubicin, and vincristine in the ABCB1 (P-glycoprotein, P-gp) overexpressing cells KBv200 and MCF-7/adr, but not in the ABCB1 negative parental cell lines KB and MCF-7. However, FG020326 did not alter the cytotoxicity of the aforementioned drugs in ABCC1 (MRP1), ABCC4 (MRP4), ABCG2 (BCRP) and LRP overexpressing cell lines, KB-CV60, NIH3T3/MRP4-2, S1-M1-80 and SW1573/2R120, respectively. FG020326, following p.o. administration, was present in concentrations sufficient for reversal of MDR in mice. The co-administration of FG020326 with paclitaxel or vincristine significantly enhanced the antitumor activity of these drugs without significantly increasing toxicity in the mice bearing the KBv200 cell xenografts. In addition, FG020326, at concentrations that reversed MDR, did not significantly affect the activity of CYP 3A4 or alter the pharmacokinetic profile of paclitaxel after co-administration with paclitaxel. FG020326 produced a significant concentration-dependent displacement of [^{3}H]-azidopine and inhibition of efflux of drug from cells. Furthermore, FG020326 was colocalized with ABCB1 in cell membranes. Hence, FG020326 is characterized as a third generation MDR modulator that holds great promise for the treatment of cancer patients with ABCB1 mediated MDR.

Keywords

FG020326; Multidrug resistance; P-glycoprotein; ABC transporter; chemosensitivity

Corresponding author: Tel:+86-20-8734-3163; Fax:+86-20-8734-3170; fulw@mail.sysu.edu.cn (LW. Fu) or Tel: 1-718-990-1432; Fax: 1-718-990-1877; chenz@stjohns.edu (ZS. Chen).
Note: Chun-ling Dai, Yong-ju Liang, Li-ming Chen and Xu Zhang contributed equally to this work.

1. Introduction

Multidrug resistance (MDR) is one of the most common causes of relapse in cancer chemotherapy. MDR can result from the overexpression of ATP-binding cassette (ABC) transporters, such as P-glycoprotein (ABCB1/P-gp), multidrug resistance proteins (ABCCs/MRPs) and breast cancer resistant protein (ABCG2/BCRP). ABC transporters promote the active efflux of the structurally and functionally diverse amphipathic anticancer drugs from cancer cells [1–3] , which can result in a decrease in the intracellular accumulation of the drug and potentially produce resistance. In fact, ABCB1 coded by *mdr1* is the most well characterized and most important mediator of MDR [4,5].

The inhibition of ABCB1 as a strategy to reverse MDR in cancer chemotherapy has been studied extensively, but the results have been equivocal [6,7]. Based on current findings, MDR modulators/inhibitors have been categorized as being 1–3 generations based on their action and interaction with traditional chemotherapeutic agents [6,8,9]. The first generation of ABCB1 modulators were identified as substrates of ABCB1 and they competitively inhibited the efflux of various antineoplastic agents by ABCB1 [10]. However, high serum concentrations of these compounds were required to reverse MDR *in vivo* thereby increased the likelihood of adverse effects. The second-generation of ABCB1 modulators displayed a superior pharmacologic profile compared to the first-generation compounds. For example, these agents could reverse MDR *in vitro* as well as *in vivo*. However, they significantly inhibited the CYP 3A4, which led to a decrease in the metabolism of various antineoplastic agents, producing unacceptable toxicity as well as dose reduction [11]. Therefore, the second generation of ABCB1 modulators has a limited use in the clinic. The third generation ABCB1 modulators potently reverse ABCB1-mediated MDR *in vivo* and *in vitro*. However, they do not significantly alter the enzymatic activity of CYP3A4 and the pharmacokinetic profile of conventional chemotherapeutic agents at clinically relevant concentrations [6,12,13]. Recent clinical studies suggest that the third-generation MDR modulators such as Tariquidar (XR9576), Zosuquidar (LY335979), Laniquidar (R102933), ONT-093 (OC144–193), and GF120918 may be effective in certain patients with MDR [13–17].

The exploratory imidazole library for the MDR project was designed around structural characteristics of known P-gp substrates and modulators: hydrophobic compounds with multiple amine groups. As such, we synthesized a novel class of triaryl-substituted imidazoles through the use of combinatorial chemistry and structure-activity relationships [18]. Among the newly synthesized triaryl-substituted imidazole derivatives screened, FG020326, 2-[(4-Methyl-trans-acrylate) phenyl]-4, 5-bis- (4-N, N-methyl- isopropyl- aminophenyl)-1(H)-imidazole, is more potent to reverse MDR in tumors associated with cancer chemotherapy [9]. In this study, we examined the efficacy of FG020326 to reverse MDR *in vitro* and *in vivo*. In addition, in mice, the plasma levels of FG020326 were determined as well as the effect of FG020326 on the plasma levels of placlitaxel.

2. Materials and Methods

2.1. Materials

FG020236 was synthesized, and isolated in the powder form using chromatography with a purity of >98%, and solved in dimethyl sulfoxide (DMSO). The molecular structure of FG020326 was shown in Fig. 1A. Paclitaxel, doxorubicin (Dox) , vincrinstine (VCR) , topotecan, Rhodamine 123 (Rho 123) and 1-(4, 5-dimethylthiazol-2-yl)-3, 5-diphenylformazan (MTT) were purchased from Sigma Chemical Co (St. Louis, MO). Dulbecco's modified Eagle's medium (DMEM) and RPMI-1640 were products of Gibco BRL from Genewindows Co. (Guangzhou, China). [^{3}H]azidopine was purchased from Amersham

Pharmacia Biotech Co. (Piscataway, NJ). Monoclonal antibody C-219 (against ABCB1) was acquired from Signet Laboratories Inc. (Dedham, MA). Monoclonal antibody ABCB1 (sc-8313) was products of Santa Cruz Biotechnology Inc from Genetime Co. (Guangzhou, China).

2.2. Cell lines and cell culture

The following cell lines were cultured in DMEM or RPMI 1640 containing 10% FBS at 37° C in a humidified atmosphere of 5% CO_2: the human breast carcinoma cell lines MCF-7 and its doxorubicin-selected derivative ABCB1 overexpressing MCF-7/adr [19]; the human oral epidermoid carcinoma cell lines KB and its VCR-selected derivative ABCB1 overexpressing KBv200 [20]; the human epidermoid carcinoma cell lines KB-3-1 and its VCR-selected derivative ABCC1 overexpressing KB-CV60 [21]; murine fibroblasts cell line NIH3T3 and the ABCC4-transfected derivative ABCC4 stable expressing NIH3T3/MRP4-2 [22]; the colon carcinoma cell line S1 and its mitoxantrone (MX)-selected derivative ABCG2 overexpressing S1-M1-80 [23,24]; the human lung squamous carcinoma cell line SW1573 and its doxorubicin-selected derivative LRP overexpressing SW1573/2R120 [25,26].

2.3. *In vitro* cytotoxicity test

The MTT assay was used to assess cytotoxicity [9,20]. In detail, cells were grown in 96-well microtiter plates. To determine the toxicity of FG020326, various concentrations of FG020326 were added into the wells. To test the effect of FG020326 on the chemosensitivity of cancer cells, FG020326 was added with full-range concentrations of 1) Dox, VCR, paclitaxel and *cis*platin (DDP) in MCF-7, MCF-7/adr, KB, and KBv200 cells, respectively; 2) Dox in SW1573 and SW1573/2R120 cells; 3) paclitaxel in KB-3-1 and KB-CV60 cells; 4) 6-MP in NIH3T3 and NIH3T3/ABCC4-2 cells; and 5) topotecan in S1 and S1-M1-80 cells. The concentrations required to inhibit growth by 50% (IC_{50}) were calculated from survival curves using the Bliss method [27]. The degree of resistance was calculated by dividing the IC_{50} of the MDR cells by that of the parental sensitive cells. The degree of the reversal of MDR was calculated by dividing the IC_{50} of the chemotherapeutic agents in the absence of FG020326 by that obtained in the presence of FG020326.

2.4. Experimental animals

Athymic nude mice were used for the KBv200 cell xenografts. NIH mice were utilized in the experiments of pharmacokinetics of FG020326 and the interaction of both FG020326 and paclitaxel. All mice were obtained from the Center of Experimental Animals, Sun Yat-sen University, maintained and reared in the Center. Female or male mice of 5–6 weeks old, weighting 20–25 g, were used for all experiments. All experiments were carried out in accordance with the guidelines on animal care and experiments of Laboratory Animals of Center of Experimental Animals, Sun Yat-sen University, and approved by Ethics Committee for animal experiments.

2.5. MDR human carcinoma xenografts

The KBv200 cell xenograft model was established as described by Chen et al [28]. Briefly, KBv200 cells grown *in vitro* were harvested and implanted subcutaneously (s.c.) under the shoulder in the nude mice. When the tumors reached a mean diameter of 0.5 cm, the mice were randomized into 4 groups and treated with various regimens including: 1) saline (q2d×6), 2) VCR (0.2 mg/kg i.p., q2d×6); 3) FG020326, 100 mg/kg, p.o., q2d×6, and 4) VCR (0.2 mg/kg, i.p., q2d×6) + FG020326 (100 mg/kg, p.o., q2d×6 given 1 h before VCR). In another experiment, animals were given the following treatments: saline (control), paclitaxel (18 mg/kg i.p. q5d×3), FG020326 (100 mg/kg, p.o., q5d×3), and paclitaxel (18 mg/kg, i.p., q5d×3) + FG020326 (100 mg/kg, p.o., q2d×6, 1 h before paclitaxel).

The body weight of the animals was measured every 3 days. The two perpendicular diameters (A and B) were recorded every 3 days and tumor volume (V) was estimated according to the formula [28]:

$$V=\frac{\pi}{6}\frac{(A+B)^3}{2}$$

The curve of tumor growth was drawn according to tumor volume and time of implantation. The mice were anesthetized and killed when the mean of tumor weights was over 1 g in the control group. Tumor tissue was excised from the mouse and its weight was measured. The rate of inhibition (IR) was calculated according to the formula [28]:

$$IR(\%)=1-\frac{\text{Mean tumor weight of experimental group}}{\text{Mean tumor weight of control group}}\times 100\%$$

2.6. Determination of FG020326 plasma levels in mice

NIH mice were divided randomly into groups according to their body weight. Each group consisted of three female and three male mice. The mice in the experimental groups were treated with FG020326 (100 mg/kg p.o.) and mice in control group received an equal volume of vehicle. Blood was collected from the retro-orbital plexus and placed in cold heparin-coated glass tubes. The blood from one male and one female mouse were pooled to ensure a quantity sufficient for detection and the plasma was isolated. Blood samples were collected at 5, and 30 min, 1, 1.5, 2, 3, 3.5, 4, 5, 6, 8, 12, and 16 h after the administration of FG020326. The plasma samples of FG020326 were measured by RP-HPLC as described previously [29].

2.7. CYP3A4 assays

Human liver tissue was obtained from Cancer Center, Sun Yat-sen University under protocols approved by the Ethics Review Committee for the conduct of human research. Microsomes were prepared by differential centrifugation and the protein concentration was determined by the Bradford method [30]. The activity of CYP3A4 was determined using nifedipine (substrate of CYP3A4) and HPLC analysis as previously described [8], with the following modification: the column temperature was 12°C instead of ambient temperature and a Hypersil ODS C_{18} column (5 μm, 150 mm×4.6 mm) instead of an octyldecylsilyl (C_{18}) reverse-phase HPLC column (3 μm, 80 mm×6.2 mm). The liver microsomes were incubated with nifedipine (50 μM) in the presence or absence of FG020326 and troleandomycin, an inhibitor of CYP3A4, as the positive control.

2.8. Determination of paclitaxel plasma levels in mice

The plasma levels of paclitaxel were determined in mice treated with paclitaxel (18 mg/kg, i.v.) or paclitaxel (18 mg/kg, i.v.) + FG020326 (100 mg/kg, p.o.). NIH mice were randomly divided into groups according to weight, with each group consisting of 6 mice (three males and three females). Mice were treated with either 100 mg/kg of FG020326 (p.o.) or vehicle on days 1 and 2. All mice were injected with 18 mg/kg of paclitaxel (10 ml/kg) via the caudal vein on day 2 one hour after FG020326 or vehicle. Blood was collected from the retro-orbital plexus and placed in cold heparin coated glass tubes. The blood from 1 male and 1 female mice were pooled and the plasma was isolated. The plasma levels of paclitaxel were analyzed by HPLC as previously described [31].

2.9. Dox accumulation and efflux

The intracellular accumulation of Dox was determined as previously described [20]. KB and KBv200 cells (in logarithmic growth phase) were treated with FG020326 (0.625, 1.25, 2.5, 5 or 10 μM) or vehicle at 37°C for 2 h in the medium. Subsequently, 10 μM Dox was added and the incubation continued for an additional 3 h. The cells were then collected, centrifuged and washed 3 times with cold PBS. The cells were resuspended in 0.3 mM HCl in 60% of ethanol. Following centrifugation, the supernatant was removed and assayed spectrofluorometrically at λ_{ex} 470 nm and λ_{em} 590 nm. FG020326 did not affect the absorbance or emission spectra of Dox.

To measure drug efflux, cells were incubated in RPMI 1640 medium containing 10% FBS at 37°C. Then the cells were treated with 10 μM Dox for 3 h at 37°C, and then incubated in the presence or absence of FG020326 at the indicated times at 37°C, harvested and quantified as described above [20].

2.10. Function analysis of ABCB1

The activity of ABCB1 was determined using the ABCB1 substrate and fluorophore Rho 123. KB and KBv200 cells were incubated for 1 h at 37°C in 5% CO_2 in the absence or presence of FG020326. After incubation, 200 ng/mL of Rho 123 was added. A sample was taken at t = 0 min to correct for background fluorescence and at t = 75 min to measure intracellular Rho 123 retention. The relative value of Rho 123 retention was identified by dividing the Rho 123 level for each measurement by that obtained in the absence of FG020326 in the ABCB1 expressing KBv200 cells [27].

2.11. [^{3}H]azidopine photoaffinity labeling of ABCB1

KBv200 cell membranes were prepared and the experiment was carried out as described [20]. Membranes (15 μg protein) were incubated with FG020326 (0.625~10 μM) for 25 min in the dark, followed by a similar incubation with 0.6 μM [^{3}H]azidopine. After UV irradiation for 2 min, the photolabeled membranes were subjected to SDS-PAGE on an 8 % gel, followed by fluorography. The presence of ABCB1 was confirmed by Western blotting using the monoclonal antibody C219 (1:1000) and ECL detection.

2.12. ATPase assay of ABCB1

The drug-efflux function of ABCB1 is linked to ATP-hydrolysis which is stimulated in the presence of ABCB1 substrates. The Vi-sensitive ATPase activity of ABCB1 in the membrane vesicles of High Five insect cells was measured as previously described [32]. The membrane vesicles (10 μg) were incubated in ATPase assay buffer (50 mM MES, pH 6.8, 50 mM KCl, 5 mM sodium azide, 2 mM EGTA, 2 mM dithiothreitol, 1 mM ouabain, and 10 mM $MgCl_2$) with or without 0.3 mM vanadate at 37°C for 5 min, then incubated with different concentrations of FG020326 at 37°C for 3 min. The ATPase reaction was induced by the addition of 5 mM Mg-ATP, and the total volume was 0.1 ml. After incubated at 37°C for 20 min, the reactions were stopped by loading 0.1 ml of 5% SDS solution. The liberated Pi was measured as described [32,33].

2.11. Expression of ABCB1

After treatment with FG020326 for 48 h, KBv200 cells were harvested and rinsed twice with PBS. Cell extracts were prepared with buffer (1× PBS, 1% Nonidet P-40, 0.5% sodium deoxycholate, 0.1% SDS, 100 μg/ml phenylmethylsulfonyl fluoride, 10 μg/ml aprotinin, 10 μg/ml leupeptin) for 30 min with occasional rocking and clarified by centrifugation at 12,000 × g for 15 min at 4°C. Identical amounts (100 μg of protein) of cell lysates were boiled for 10 min and resolved by sodium dodecyl sulfate polycrylamide gel electrophoresis (SDS-PAGE)

and electrophoretically transferred onto PVDF membranes. After being incubated in blocking solution containing 5% non-fat milk in TBST buffer (10 mM Tris-HCL (pH 8.0), 150 mM NaCl, and 0.1% Tween 20) for 2 h at 4°C, membranes were incubated with the appropriately diluted primary antibody. The expression of β-actin was used as loading control. The membranes were then incubated for 1 h with HRP-conjugated secondary antibody at 1:1000 dilutions. Proteins were detected by the enhanced chemiluminescence detection system (Amersham, Aylesbury, UK). Protein expression was quantified by Scion Image software (Scion Co, USA) [34].

2.12. Localization of FG020326 in cells by confocal microscopy

FG020326 is an auto-fluoresce compound. KBv200 cells were incubated at 37°C for 5 h with 5 μM FG020326. Cells were collected following treatment with trypsin and washed twice with PBS. Subsequently, cells were incubated with an ABCB1-specific monoclonal antibody (UIC2) directly conjugated to PE for 0.5 h at room temperature. After washing three times with PBS, cells were mounted on microscope slides and visualized under a confocal microscope (Olympus FV1000) and digital images were recorded.

2.13. Statistical analysis

All experiments were repeated at least 3 times and the differences were determined by using the Student's t-test. The significance was determined at $p < 0.05$.

3. Results

3.1. Reversal of MDR by FG020326 *in vitro*

As shown in table 1, MCF-7/adr cells exhibited 176-, 68-, and 49-fold resistance to Dox, VCR, and paclitaxel, respectively, compared with the parental MCF-7 cells. KBv200 cells were 49-, 47-, and 35-fold resistance to Dox, VCR, and paclitaxel, respectively, compared with the parental KB cells. Comparison of S1 cells, S1-M1-80 cells were 143.2-fold resistant to topotecan. KB-CV60 cells were 12-fold resistant to VCR compared with the parental KB-3-1 cells. SW1573/2R120 cells were 13-fold resistant to doxorubicin compared with its parental SW1573 cells and NIH3T3/MRP4-2 cells were 22-fold resistant to VCR compared with its parental NIH3T3 cells.

Prior to examining the efficacy of FG020326 to reverse ABCB1-, ABCC1-, ABCC4-, ABCG2- and LRP -mediated MDR in cancer cells, we first assessed the cytotoxicity of FG020326 in different cell lines by using the MTT assay. The IC_{50} values of FG020326 for the entire cell lines tested were > 50 μM. Cell survival was > 90% in all cell lines under the concentrations used in this experiment to reversal MDR (Data not shown). FG020326 at 1.25, 2.5 and 5.0 μM produced a concentration-dependent increase in the cytotoxicity of Dox, VCR and paclitaxel in MDR cells overexpressing ABCB1, including MCF-7/adr and KBv200 cells (Table 1). However, FG020326 had neither significant effect on the enhancement of drug cytotoxicity in the parental sensitive cells, including MCF-7, KB, KB-3-1, NIH3T3, S1 and SW1573 cells, nor on the reversal of MDR induced by ABCC1, ABCC4, ABCG2 and LRP (Table 1). In addition, FG020326 did not significantly alter the IC_{50} values of 5-fluoropyrimidine (5-FU) and cisplatin which are not substrates of ABCB1 in ABCB1 expressing MDR cells (Table 1).

3.2. Reversal of MDR by FG020326 in KBv200 cell xenografts

The xenograft model of KBv200 cells was used to determine the ability of FG020326 to reverse MDR *in vivo*. As shown in Figure 1, the results indicated that neither FG020326 nor paclitaxel, VCR alone had any significant effect on the growth of the xenograft model of KBv200 cells (P>0.05 *versus* the saline control group). However, the combination of FG020326 and VCR

or paclitaxel produced a significantly inhibitory effect on the growth of the xenografts (Fig. 1B and 1C; Fig S1), and the inhibition rate was 46.7% or 51.7% (Table 2), respectively ($P<0.05$ *versus* the control group, or FG020326 alone group or VCR alone and paclitaxel alone group, respectively). In addition, no mortality or decrease in body weight was associated with the combination treatments (Table 2), suggesting that the combination regimen did not result in increased toxicity.

3.3. Plasma levels of FG020326 in mice

To further confirm whether FG020326 could achieve plasma levels required to reverse MDR *in vivo*, we measured the plasma levels in NIH mice following its p.o. administration. The p.o. administration of 100 mg/kg of FG020236 produced a peak plasma concentration of 5.3 μM (Fig. 1D). In addition, a plasma concentration of > 1.24 μM of FG020236 was obtained at 8 h after administration. Furthermore, the concentration of FG020326 was still sufficient (0.92 μM) to reverse drug resistance at 12 h after the p.o. administration of FG020326. However, at the same time point, paclitaxel and Dox were almost completely metabolized [8,35,36]. These suggested that FG020326 could achieve the concentration that could potently reverse MDR *in vivo* and keep long time enough to enhance the action of conventional chemotherapeutic drugs under the doses used to treat nude mice with xenograft.

3.4. Effect of FG020236 on the activity of human hepatic CYP 3A4

Numerous reports indicate that there is a considerable overlap in the tissue distribution and substrate preference between ABCB1 and CYP3A4 [37–39]. To identify FG020326 whether belongs to the third generation MDR modulator, we determined its effect on human liver microsomal CYP3A4 *in vitro*. Troleandomycin, a potent inhibitor of CYP 3A4, significantly inhibited the activity of CYP 3A4 in a concentration-dependent manner. However, FG020326 only produced a significant inhibition of CYP3A4 at 25 μM (Fig. 2A), which is significantly higher than that required to reverse MDR *in vitro*.

3.5. Effect of FG020326 on the pharmacokinetics of paclitaxel in mice

The effect of FG020236 on the pharmacokinetic profile of paclitaxel is illustrated in Figure 2B. The administration of FG020236 did not significantly alter the plasma levels of paclitaxel compared to vehicle-treated animals. There was no significant difference in the pharmacokinetic parameters of paclitaxel between vehicle- and FG020236-treated mice (Table 3). These results suggest that FG020326 had no apparent effect on paclitaxel pharmacokinetics.

3.6. Effect of FG020326 on the intracellular accumulation of Dox

Baseline experiments indicated that the intracellular accumulation of Dox in KBv200 cells was only approximately one–fourth of that of KB cells. After KBv200 and KB cells were exposed to 0.625, 1.25, 2.5, 5 or 10 μM FG020326, Dox accumulation was significantly enhanced in KBv200 cells by 1.4-, 2.1-, 2.6-, 3.0- and 3.7-fold, respectively. However, in the drug sensitive KB cells, FG020236 did not significantly alter the intracellular accumulation of Dox (Fig. 3A).

Subsequently, we performed experiments to determine whether the increased accumulation of Dox in the KBv200 cells caused by FG020326 was due to inhibition of Dox efflux. The time course of Dox efflux after 2 h of accumulation is shown in Figure 3B. The KBv200 cells released a significantly high percentage of intracellularly accumulated Dox compared to KB cells. For example, at 30 min, 58% of the accumulated Dox was effluxed from the KBv200 cells, compared to only 28% from KB cells. FG020326 (5 μM) significantly inhibited the efflux of Dox from the KBv200 cells, but not the KB cells (Fig. 3B).

The incubation of KBv200 cells with 1.25, 2.5 or 5 μM FG020326 for 2 h significantly increased Rho 123 accumulation in a dose-dependent manner. However, the accumulation of Rho 123 in the drug sensitive KB cells was not significantly altered by the addition of FG020326 (Fig. 3C).

3.7. Photolabeling of ABCB1 with [^{3}H]azidopine, ATPase assay of ABCB1, expression of ABCB1, and localization of FG020326 in membrane of KBv200 cells

The direct interaction of FG020326 with ABCB1 in KBv200 cell membranes was assessed by examining its ability to prevent the binding of the ABCB1 photoaffinity label [^{3}H]azidopine. FG020326 produced a significant concentration-dependent inhibition of [^{3}H]azidopine labeling to ABCB1 (Fig. 4A).

It is known that the efflux function of ABCB1 is coupled to ATP hydrolysis by the ATPase domains that are activated in the presence of ABCB1 substrates [33]. The second generation MDR modulator, a substrate of ABCB1, often induced an increase of the ATPase activity of ABCB1. Therefore, we examined the effect of FG020326 on ATPase activity in isolated membrane vesicles of High five insect cells. As shown in Figure 4B, FG020326 resulted in a significant concentration-dependent inhibition of ATPase activity, with an IC_{50} value of 2.5 μM. This suggests that FG020326 maybe not a substrate of ABCB1 and belongs to the third generation MDR modulator.

The reversal of ABC transporters mediated MDR can be achieved either by decreasing their expression or by inhibiting their function. To study the effect of FG020326 on ABCB1 expression, KBv200 cells were incubated with FG020326 and expression level of protein in ABCB1 transporters was examined by Western blot. The results showed that no marked difference of the expression level of protein of ABCB1 was observed in the cells treated by FG020326 for 48 h (Fig. 4C). These results provide further evidence of the regulatory mechanisms that are not involved in decreasing the expression of ABCB1 by FG020326 in the reversal of MDR.

To further confirm whether FG020326 is directly bound to ABCB1, the localization of FG020326 was determined using confocal microscopy. The results, as shown in Figure 4D, indicated the co-localization of FG020326 and ABCB1 in the plasma membrane of KBv200 cells. This implies FG020326 directly binds to ABCB1 transporter.

4. Discussion

Resistance to drug therapy remains a major challenge in cancer chemotherapy. Cellular drug efflux mediated by ABC transporters is thought to play an important role. ABCB1 (P-gp), one of the most extensive and important drug transporter [1,40,41], has been investigated in clinic and high ABCB1 expression and activity have been reported to be associated with poor clinical outcome in cancer patients [41–43]. Based on these findings a rationale was developed for modulation of ABCB1 activity as a therapeutic approach [10,44]. Simultaneous genetic knockout of *mdr1a* and *mdr1b* resulted in healthy mice, indicating that ABCB1 is not essential for basic physiological functions [45]. This suggested that the combination of anticancer drugs with a non-toxic and potent ABCB1 inhibitor may be a promising strategy to solve the problem of resistance. Randomized trials with first-generation ABCB1 inhibitors such as cyclosporin A, quinidine or verapamil were largely inconclusive because of unexpected interactions affecting pharmacokinetics of the cytostatic agents and adverse side effects [6]. Subsequently, administration of the second-generation inhibitor valspodar with a more favourable pharmacological profile failed to achieve clinical benefits [46–49]. One reason that was considered to explain this failure was the fact that most of the second generation inhibitors of ABCB1 also interact with CYP 3A4 that significantly affect the pharmacokinetic profile

including AUC and excretion of chemotherapeutic agents, thus leading to unacceptable toxicity. This in turn led to consideration of developing new third generation of ABCB1 inhibitors, which potentially reverse the MDR *in vitro* and *in vivo* without affecting the CYP3A4 activity and pharmacokinetic profile of chemotherapeutic agents.

Among modulators of MDR under investigation, some are specific for a single transporter. For example, valspodar, XR9576, GF120918, LY335979 and ONT-093 are inhibitors for ABCB1 only [11,12,43,46,50]; MK571 and probenecid are for ABCC1 only; FTC is a specific inhibitor of ABCG2. Other modulators inhibit more than one ABC drug transporter. For example, verapamil, cyclosporine A and MS-209 are modulators for ABCB1 and ABCC1 while biricodar is a chemosensitizer for ABCB1, ABCC1 and ABCG2 [43]. As shown in Table 1, the *in vitro* potency of FG020326 was evaluated by MTT assay. FG020326 significantly enhanced sensitivity of ABCB1 expressing MCF-7/adr and KBv200 cells to conventional chemotherapeutic agents such as Dox, VCR, paclitaxel in a dose-dependent manner, but not in the enhancement of potency of ABCB1 substrate cytotoxic drugs in non-ABCB1-expressing parental cell lines and the activity of reversal MDR induced by ABCC1, ABCC4, LRP and ABCG2 (Table 1). These studies clearly indicated FG020326 specifically targeted to ABCB1 and reversed ABCB1-mediated MDR.

The ongoing search for MDR modulators that can be applied in the clinic is into its third generation. Since the initial study from Tsuruo and colleagues that verapamil could reverse ABCB1-mediated MDR was reported, a large number of compounds which can reverse the ABCB1-mediated MDR phenotype have been described. However, the application of ABCB1 reversing agents in combination with conventional chemotherapy has limited to success. So far, the second and third generation modulators, some of which are in clinical trials were drawn from chemical derivatization of first-generation molecules and from combinatorial chemistry designed for the most against ABCB1. Prominent examples are biricodar, valspodar, XR9051, XR9576, MS-209, R101933, LY335979 and ONT-093 [11,12,43,46,50]. These modulators are more potent and less toxic than first-generation modulators; some are still prone to adverse effects, poor solubility, and unfavorable changes in pharmacokinetics of the anticancer drugs and limited clinical benefit. These have spurred on efforts to search for more effective compounds with not interaction with conventional chemotherapeutic agents. New agents (the third generation MDR modulators) developed specifically to inhibit drug transporter and modulate MDR are still currently one of the most important strategies in the field of cancer chemotherapy.

In vitro, FG020326 had potent MDR-reversing activity in ABCB1-mediated MDR cells at the concentration which by itself is not cytotoxic. Treatment of KBv200 tumor-bearing Balb/c mice with either VCR/paclitaxel or FG020326 alone had no effect on the growth rate of tumors. However, co-administration of FG020326 with VCR or paclitaxel significantly reduced the growth rate of the KBv200 cell xenografts ($P<0.05$). Moreover, there was no substantial or reproducible increase in body weight loss in mice treated with VCR or paclitaxel plus FG020326 compared with drug alone groups (Fig. 1B and 1C; Table 2). Taking into account the dose-related problems with the first-generation modulators, we deliberately set out to test whether FG020326 achieves sufficient plasma concentrations and stable enough time for reversing of MDR in mice. The plasma peak concentration of FG020326 was about 5.3 μM and not less than 1.24 μM until 8 h following FG020326 administration (p.o) at 100 mg/kg (Fig. 1D). This suggests the concentrations of FG020326 sufficient to inhibit the function of ABCB1 may be achieved and keep long enough to meet the reversal of MDR *in vivo*. Furthermore, many of the anticancer drugs are substrates for both ABC transporters and CYP 3A4. Most of the second-generation MDR chemosensitizers are also substrates of CYP 3A4 and inhibit CYP 3A4 activity which may result in unpredictable pharmacokinetic interactions. Co-administration of an MDR modulator may significantly elevate plasma concentrations of

an anticancer drug by interfering with its clearance. This would increase the concentration of an anticancer drug leading to unacceptable side effects, necessitating dose reductions down to pharmacologically ineffective levels [38]. Because of these problems, MDR modulators have not improved the therapeutic efficiency of anticancer drugs unless such novel MDR modulators lack significant inhibition of CYP 3A4 activity. FG020326 did not significantly inhibit CYP 3A4 activity until 25 μM, which was much higher than that capable of reversing MDR *in vitro*. Importantly, the profile of pharmacokinetics of paclitaxel was similar between two groups no matter treated with and without FG020326. This property may give FG020326 significant advantage for clinical administration because it was not able to affect the pharmacokinetics of anticancer drugs such as paclitaxel after co-administration of FG020326. These findings suggest that FG020326 may belong to the third-generation MDR modulators.

Similar to other ABCB1 inhibitors, FG020326 may be able to reverse ABCB1-mediated drug resistance by affecting to drug efflux. Consistent with this notion, we found that incubating MDR cells with a combination Dox and FG020326 resulted in high intracellular drug accumulation (Fig. 3A). A similar result was obtained in the accumulation of Rho 123 (Fig. 3C). Efflux of a chemotherapeutic drug from those MDR cells was significantly faster in the absence of FG020326, than in the presence of FG020326 (Fig. 3B). On the other hand, a majority of substrates which interact with the ABC transporters stimulate the ATP hydrolysis, but the fact that presence of FG020326 inhibited ABCB1 ATPase suggested that it behaved difference from the known MDR modulators. These data led us to speculate on the direct interaction of the compound with the transporters and encouraged us to confirm the direct interaction with displacement of a photoaffinity label. The inhibition of drug efflux as a result of direct interaction of FG020326 with ABCB1 was implied by the potent displacement of a photoaffinity label, [^{3}H]azidopine and co-localization of this compound and ABCB1 by confocal microscopy (Fig. 4A and 4D).

In summary, we observed an improvement in targeting ABCB1-mediated MDR reversal *in vitro* and *in vivo* when FG020326 was co-administered with a conventional anticancer drug. FG020326 could achieve plasma concentrations capable of reversing MDR *in vitro* without having any effect on CYP 3A4 activity and the profile of pharmacokinetics of paclitaxel in mice. These results suggest that FG020326 is the third generation of specifically targeting ABCB1 that holds promising clinical potential. The mechanism of MDR modulation by FG020326 is associated with an increase in intracellular drug accumulation induced by its direct binding to ABCB1. Further studies with a dog or monkey model system will validate the use of this compound for reversal of MDR in the cancer patients.

Supplementary Material

Refer to Web version on PubMed Central for supplementary material.

Abbreviation

MDR	multidrug resistance
ABCB1, P-gp	P-glycoprotein
VCR	vincristine
Dox	Doxorubicin
VRP	verapamil
MTT	1-(4, 5-dimethylthiazol-2-yl)-3, 5-diphenylformazan
ABCC MRP	multidrug-resistance protein

LRP	lung resistant protein
ABCG2, BCRP	breast cancer resistant protein
CYP 3A4	cytochrome P450 isoenzyme 3A4

Acknowledgments

We thank Drs. S.E. Bates, and R.W. Robey (NCI, NIH) for S1 and S1-M1-80 cell lines; Dr. G.D. Kruh (Fox Chase Cancer Center, Philadelphia) for the cDNA of human ABCC4. We thank Yangmin (Mimi) Chen (Montgomery High School, New Jersey) for the editorial assistance. This work was supported by the grants from Chinese National Natural Sciences Foundation (No. 30672407 L-W. Fu and No. 30600769 L-M. Chen,), Chinese Ministry of Education Doctor Foundation (No. 20050558062 L-W. Fu) and St. John's University Faculty Start-Up Funding (No. C-0531, Z-S. Chen). Drs. C-P Wu and SV Ambudkar were supported by the Intramural Research Program of the NIH, National Cancer Institute, Center for Cancer Research.

REFERENCES

1. O'Connor R. The pharmacology of cancer resistance. Anticancer Res 2007;27:1267–1272. [PubMed: 17593618]
2. Donnenberg VS, Donnenberg AD. Multiple drug resistance in cancer revisited: the cancer stem cell hypothesis. J Clin Pharmacol 2005;45:872–877. [PubMed: 16027397]
3. Sparreboom A, Danesi R, Ando Y, Chan J, Figg WD. Pharmacogenomics of ABC transporters and its role in cancer chemotherapy. Drug Resist Updat 2003;6:71–84. [PubMed: 12729805]
4. Ambudkar SV, Kimchi-Sarfaty C, Sauna ZE, Gottesman MM. P-glycoprotein: from genomics to mechanism. Oncogene 2003;22:7468–7485. [PubMed: 14576852]
5. Perez-Victoria JM, Di Pietro A, Barron D, Ravelo AG, Castanys S, Gamarro F. Multidrug resistance phenotype mediated by the P-glycoprotein-like transporter in Leishmania: a search for reversal agents. Curr Drug Targets 2002;3:311–333. [PubMed: 12102602]
6. Krishna R, Mayer LD. Modulation of P-glycoprotein (PGP) mediated multidrug resistance (MDR) using chemosensitizers: recent advances in the design of selective MDR modulators. Curr Med Chem 2001;1:163–174.
7. Sikic BI, Fisher GA, Lum BL, Halsey J, Beketic-Oreskovic L, Chen G. Modulation and prevention of multidrug resistance by inhibitors of P-glycoprotein. Cancer Chemother Pharmacol 1997;40:S13–S19. [PubMed: 9272128]
8. Dai CL, Xiong HY, Tang LF, Zhang X, Liang YJ, Zeng MS, et al. Tetrandrine achieved plasma concentrations capable of reversing MDR in vitro and had no apparent effect on doxorubicin pharmacokinetics in mice. Cancer Chemother Pharmacol 2007;60:741–750. [PubMed: 17273824]
9. Chen LM, Wu XP, Ruan JW, Liang YJ, Ding Y, Shi Z, et al. Screening novel, potent multidrug-resistant modulators from imidazole derivatives. Oncol Res 2004;14:355–362. [PubMed: 15301426]
10. Sikic BI. Pharmacologic approaches to reversing multidrug resistance. Semin Hematol 1997;34:40–47. [PubMed: 9408960]
11. Krishna R, Mayer LD. Multidrug resistance (MDR) in cancer. Mechanisms, reversal using modulators of MDR and the role of MDR modulators in influencing the pharmacokinetics of anticancer drugs. Eur J Pharm Sci 2000;11:265–283. [PubMed: 11033070]
12. Thomas H, Coley HM. Overcoming multidrug resistance in cancer: an update on the clinical strategy of inhibiting p-glycoprotein. Cancer Control 2003;10:159–165. [PubMed: 12712010]
13. Muller H, Pajeva IK, Globisch C, Wiese M. Functional assay and structure-activity relationships of new third-generation P-glycoprotein inhibitors. Bioorg Med Chem 2008;16:2448–2462. [PubMed: 18083034]
14. Morschhauser F, Zinzani PL, Burgess M, Sloots L, Bouafia F, Dumontet C. Phase I/II trial of a P-glycoprotein inhibitor, Zosuquidar.3HCl trihydrochloride (LY335979), given orally in combination with the CHOP regimen in patients with non-Hodgkinɾs lymphoma. Leuk Lymphoma 2007;48:708–715. [PubMed: 17454628]

15. van Zuylen L, Sparreboom A, van der Gaast A, Nooter K, Eskens FA, Brouwer E, et al. Disposition of docetaxel in the presence of P-glycoprotein inhibition by intravenous administration of R101933. Eur J Cancer 2002;38:1090–1099. [PubMed: 12008197]
16. Guns ES, Bullock PL, Reimer ML, Dixon R, Bally M, Mayer LD. Assessment of the involvement of CYP3A in the vitro metabolism of a new modulator of MDR in cancer chemotherapy, OC144–193, by human liver microsomes. Eur J Drug Metab Pharmacokinet 2001;26:273–282. [PubMed: 11808870]
17. Kuppens IE, Witteveen EO, Jewell RC, Radema SA, Paul EM, Mangum SG, et al. A phase I, randomized, open-label, parallel-cohort, dose-finding study of elacridar (GF120918) and oral topotecan in cancer patients. Clin Cancer Res 2007;13:3276–3285. [PubMed: 17545533]
18. Ruan JW, Fu LW, Huang ZS, Chen LM, MA L, Gu LQ. Studies on synthesis of multiaryl-substituted imidazoles and reversal activity on the multidrug resistance. Chem J Chinese U 2004;25:870–873.
19. Fu L, Liang Y, Deng L, Ding Y, Chen L, Ye Y, et al. Characterization of tetrandrine, a potent inhibitor of P-glycoprotein-mediated multidrug resistance. Cancer Chemother Pharmacol 2004;53:349–356. [PubMed: 14666379]
20. Fu LW, Zhang YM, Liang YJ, Yang XP, Pan QC. The multidrug resistance of tumour cells was reversed by tetrandrine in vitro and in xenografts derived from human breast adenocarcinoma MCF-7/adr cells. Eur J Cancer 2002;38:418–426. [PubMed: 11818209]
21. Aoki S, Chen ZS, Higasiyama K, Setiawan A, Akiyama S, Kobayashi M. Reversing effect of agosterol A, a spongean sterol acetate, on multidrug resistance in human carcinoma cells. Jpn J Cancer Res 2001;92:886–895. [PubMed: 11509122]
22. Lee K, Klein-Szanto AJ, Kruh GD. Analysis of the MRP4 drug resistance profile in transfected NIH3T3 cells. J Natl Cancer Inst 2000;92:1934–1940. [PubMed: 11106685]
23. Volk EL, Farley KM, Wu Y, Li F, Robey RW, Schneider E. Overexpression of wild-type breast cancer resistance protein mediates methotrexate resistance. Cancer Res 2002;62:5035–5040. [PubMed: 12208758]
24. Litman T, Brangi M, Hudson E, Fetsch P, Abati A, Ross DD, et al. The multidrug-resistant phenotype associated with overexpression of the new ABC half-transporter, MXR (ABCG2). J Cell Sci 2000;113(Pt 11):2011–2021. [PubMed: 10806112]
25. Kubota T, Furukawa T, Tanino H, Suto A, Otan Y, Watanabe M, et al. Resistant mechanisms of anthracyclines--pirarubicin might partly break through the P-glycoprotein-mediated drug-resistance of human breast cancer tissues. Breast Cancer 2001;8:333–338. [PubMed: 11791127]
26. Slovak ML, Ho JP, Cole SP, Deeley RG, Greenberger L, de Vries EG, et al. The LRP gene encoding a major vault protein associated with drug resistance maps proximal to MRP on chromosome 16: evidence that chromosome breakage plays a key role in MRP or LRP gene amplification. Cancer Res 1995;55:4214–4219. [PubMed: 7671223]
27. Shi Z, Liang YJ, Chen ZS, Wang XW, Wang XH, Ding Y, et al. Reversal of MDR1/P-glycoprotein-mediated multidrug resistance by vector-based RNA interference in vitro and in vivo. Cancer Biol Ther 2006;5:39–47. [PubMed: 16319528]
28. Chen LM, Liang YJ, Ruan JW, Ding Y, Wang XW, Shi Z, et al. Reversal of P-gp mediated multidrug resistance in-vitro and in-vivo by FG020318. J Pharm Pharmacol 2004;56:1061–1066. [PubMed: 15285852]
29. Dai CL, Li S, Liang YJ, Liao H, Deng WJ, Yan L, Fu LW. A method for determining the concentration of FG020326 in mice plasma by RP-HPLC. Chin Pharmacol Bull 2007;23:4.
30. Bradford MM. A rapid and sensitive method for the quantitation of microgram quantities of protein utilizing the principle of protein-dye binding. Anal Biochem 1976;72:248–254. [PubMed: 942051]
31. Yonemoto H, Ogino S, Nakashima MN, Wada M, Nakashima K. Determination of paclitaxel in human and rat blood samples after administration of low dose paclitaxel by HPLC-UV detection. Biomed Chromatogr 2007;21:310–317. [PubMed: 17221932]
32. Ramachandra M, Ambudkar SV, Chen D, Hrycyna CA, Dey S, Gottesman MM, et al. Human P-glycoprotein exhibits reduced affinity for substrates during a catalytic transition state. Biochemistry 1998;37:5010–5019. [PubMed: 9538020]

33. Shi Z, Peng XX, Kim IW, Shukla S, Si QS, Robey RW, et al. Erlotinib (Tarceva, OSI-774) antagonizes ATP-binding cassette subfamily B member 1 and ATP-binding cassette subfamily G member 2-mediated drug resistance. Cancer Res 2007;67:11012–11020. [PubMed: 18006847]
34. Shi Z, Liang YJ, Chen ZS, Wang XH, Ding Y, Chen LM, et al. Overexpression of Survivin and XIAP in MDR cancer cells unrelated to P-glycoprotein. Oncol Rep 2007;17:969–976. [PubMed: 17342344]
35. Holmes FA, Rowinsky EK. Pharmacokinetic profiles of doxorubicin in combination with taxanes. Semin Oncol 2001;28:8–14. [PubMed: 11552225]
36. Danesi R, Conte PF, Del Tacca M. Pharmacokinetic optimisation of treatment schedules for anthracyclines and paclitaxel in patients with cancer. Clin Pharmacokinet 1999;37:195–211. [PubMed: 10511918]
37. Pal D, Mitra AK. MDR- and CYP3A4-mediated drug-drug interactions. J Neuroimmune Pharmacol 2006;1:323–339. [PubMed: 18040809]
38. Pal D, Mitra AK. MDR- and CYP3A4-mediated drug-herbal interactions. Life Sci 2006;78:2131–2145. [PubMed: 16442130]
39. Lin JH, Yamazaki M. Role of P-glycoprotein in pharmacokinetics: clinical implications. Clin Pharmacokinet 2003;42:59–98. [PubMed: 12489979]
40. Callaghan R, Crowley E, Potter S, Kerr ID. P-glycoprotein: So Many Ways to Turn It On. J Clin Pharmacol 2008;48:365–378. [PubMed: 18156365]
41. Ottaiano A, De Chiara A, Fazioli F, Talamanca AA, Mori S, Botti G, et al. Biological prognostic factors in adult soft tissue sarcomas. Anticancer Res 2005;25:4519–4526. [PubMed: 16334136]
42. Jamroziak K, Robak T. Pharmacogenomics of MDR1/ABCB1 gene: the influence on risk and clinical outcome of haematological malignancies. Hematology 2004;9:91–105. [PubMed: 15203864]
43. Tan B, Piwnica-Worms D, Ratner L. Multidrug resistance transporters and modulation. Curr Opinion Oncol 2000;12:450–458.
44. Ford JM, Yang JM, Hait WN. P-glycoprotein-mediated multidrug resistance: experimental and clinical strategies for its reversal. Cancer Treat Res 1996;87:3–38. [PubMed: 8886447]
45. Schinkel AH, Mayer U, Wagenaar E, Mol CA, van Deemter L, Smit JJ, et al. Normal viability and altered pharmacokinetics in mice lacking mdr1-type (drug-transporting) P-glycoproteins. Proc Natl Acad Sci USA 1997;94:4028–4033. [PubMed: 9108099]
46. Modok S, Mellor HR, Callaghan R. Modulation of multidrug resistance efflux pump activity to overcome chemoresistance in cancer. Curr Opin Pharmacol 2006;6:350–354. [PubMed: 16690355]
47. Atadja P, Watanabe T, Xu H, Cohen D. PSC-833, a frontier in modulation of P-glycoprotein mediated multidrug resistance. Cancer Metastasis Rev 1998;17:163–168. [PubMed: 9770112]
48. Greenberg PL, Lee SJ, Advani R, Tallman MS, Sikic BI, Letendre L, et al. Mitoxantrone, etoposide, and cytarabine with or without valspodar in patients with relapsed or refractory acute myeloid leukemia and high-risk myelodysplastic syndrome: a phase III trial (E2995). J Clin Oncol 2004;22:1078–1086. [PubMed: 15020609]
49. Advani R, Saba HI, Tallman MS, Rowe JM, Wiernik PH, Ramek J, et al. Treatment of refractory and relapsed acute myelogenous leukemia with combination chemotherapy plus the multidrug resistance modulator PSC 833 (Valspodar). Blood 1999;93:787–795. [PubMed: 9920827]
50. Wang RB, Kuo CL, Lien LL, Lien EJ. Structure-activity relationship: analyses of p-glycoprotein substrates and inhibitors. J Clin Pharm Ther 2003;28:203–228. [PubMed: 12795780]

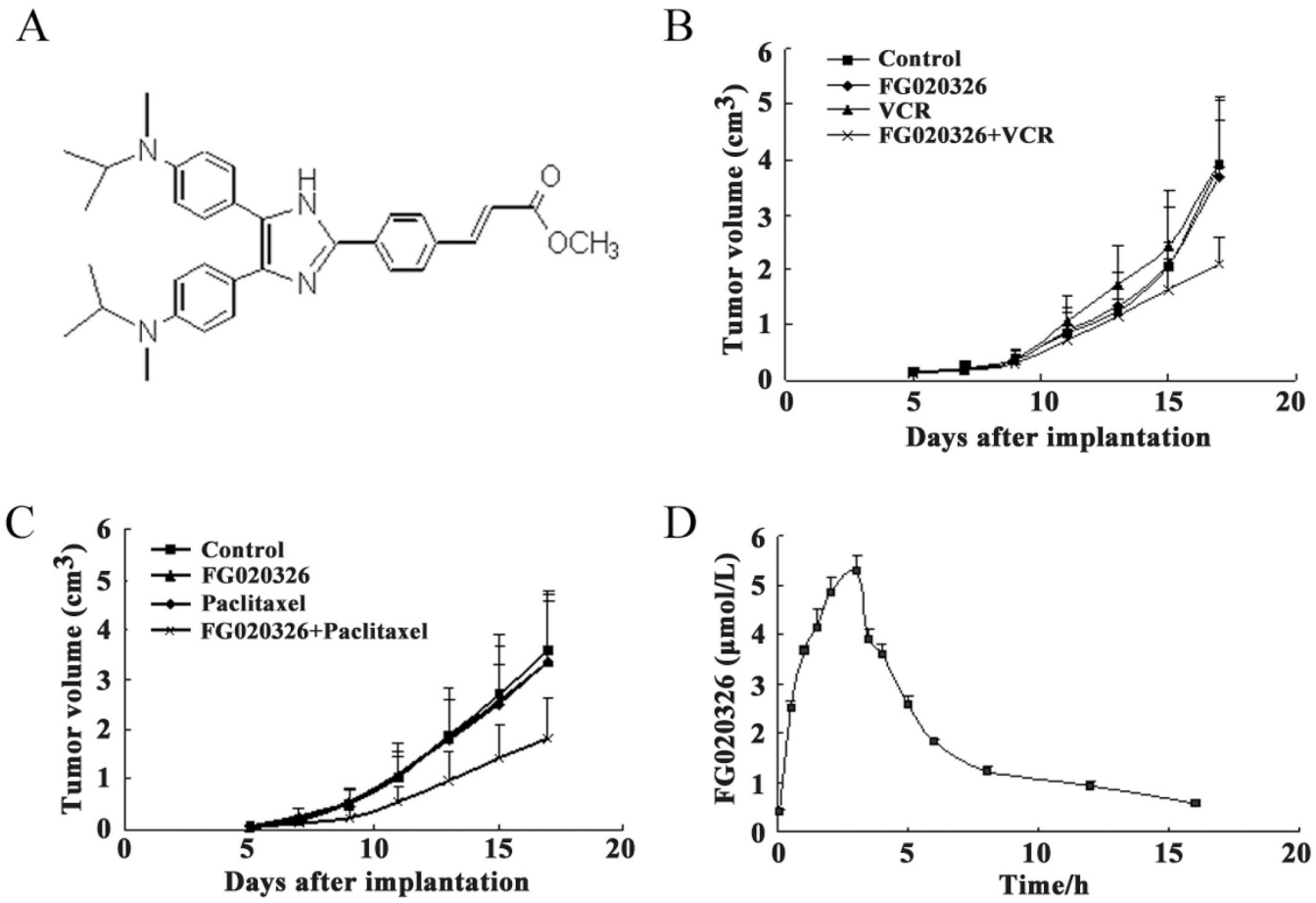

Figure 1.

The structure of FG020326 (A); Reversal of MDR *in vivo* by FG020326 (B and C), the experiment was carried out using athymic mice implanted subcutaneously (s.c.) with KBv200 cells. The treatments were administered as indicated in the "Materials and Methods". Data represent the mean tumor volume for each group ± SD in 10 mice after implantation; The pharmacokinetic study of FG020326 (D), HPLC analysis was performed as described in the "Material and Methods". The data represent the means and standard deviations of three independent experiments.

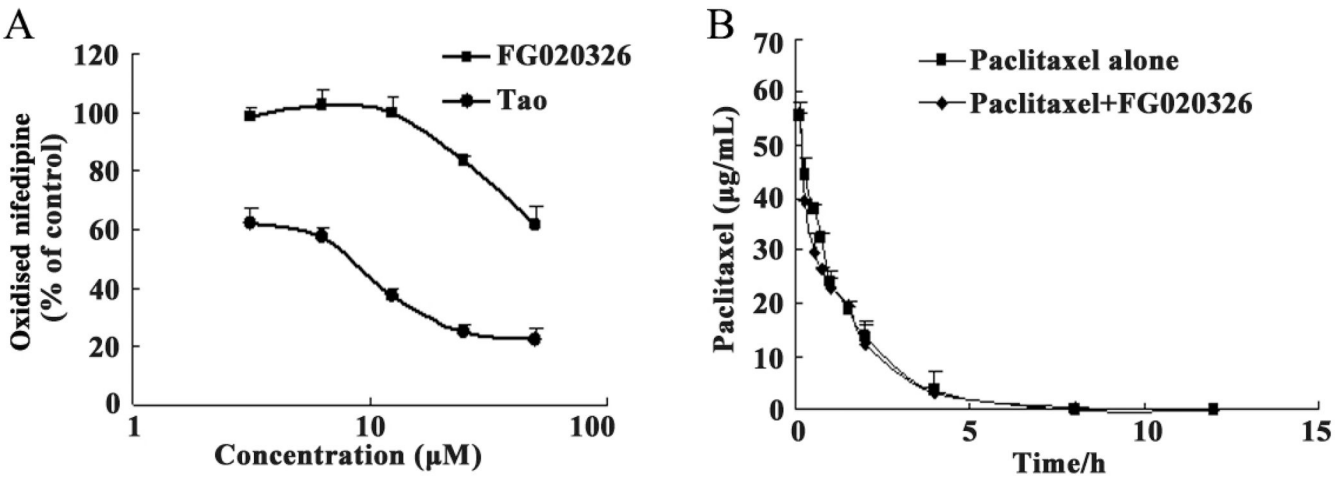

Figure 2.

The effect of FG020326 and troleandomycin on the activity of CYP 3A4 (A), Tao, troleandomycin, an inhibitor of CYP3A4, as the positive control; the effect of FG020326 on the profile of paclitaxel pharmacokinetics in mice (B). HPLC analysis was performed as described in the "Material and Methods". The data represent the means and standard deviations of three independent experiments.

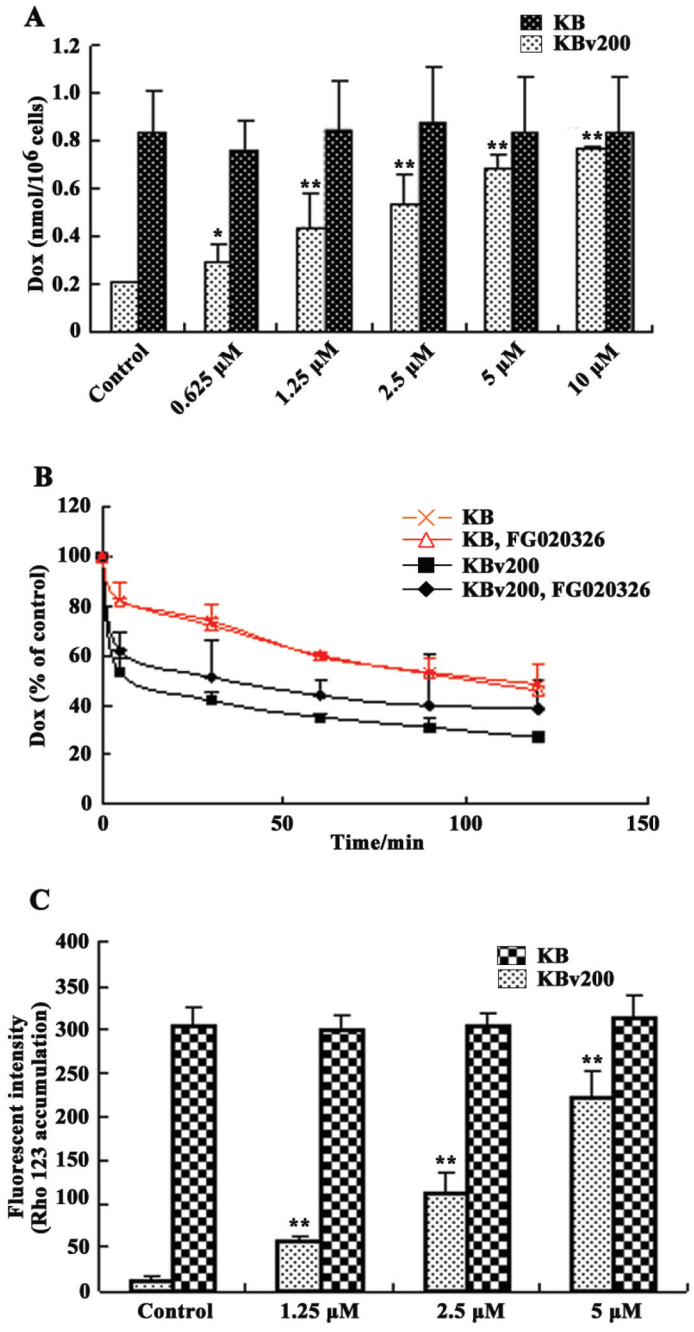

Figure 3.

Effect of FG020326 on the accumulation of Dox and rhodamine 123, and the efflux of Dox in KB and KBv200 cells. Dox accumulation (A), Rhodamine 123 accumulation (C). Bars represent means and standard deviations of triplicate determinations; * and ** represent $P<0.05$ and 0.01, respectively, compared with the control group in the KBv200 cells. Dox efflux (B). Values were expressed as percent compared with apical point.

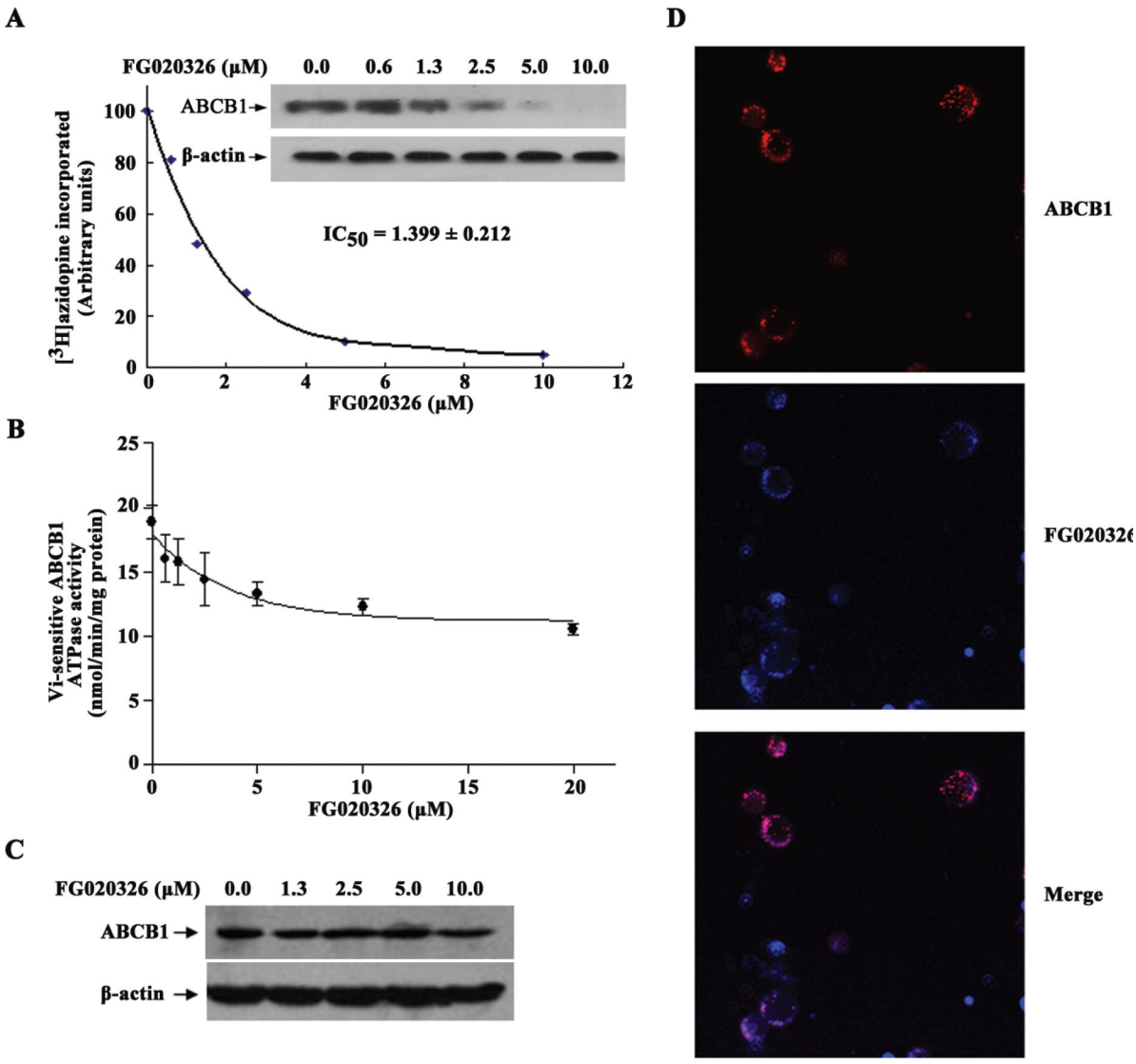

Figure 4.

Effect of FG020326 on [^{3}H]-azidopine photoaffinity labeling of ABCB1 (A), the photoaffinity labeling of ABCB1 with [^{3}H]-azidopine was performed with different concentrations of FG020326. The radioactivity incorporated into ABCB1 was determined by exposing the gel to an X-ray film at −70°C; ATPase activity of ABCB1 (B), the Vi-sensitive ATPase activity of ABCB1 in membrane vesicles was determined with different concentrations of FG020326, as described in “Materials and Methods”. The basal ATPase activity (in the absence of FG020326) was subtracted from the activities obtained at the indicated FG020326 concentrations and the graph was fitted by non-linear least-squares regression analysis using GraphPad Prism version 2.0; The expression of ABCB1 (C), equal amounts of total cell lysates were used for each sample and immunoblots were detected with western blot described as “Materials and Methods”. Experiments were repeated at least three independent times, and a representative experiment was shown; FG020326 co-localized with ABCB1 to plasma membrane (D). KBv200 cells were visualized under a confocal microscope and digital images were captured.

Table 1

Effect of FG020326 on reversing ABCB1-, ABCC1-, ABCC4-, ABCG2-, and LRP-mediated drug resistance mediated drug resistance

	IC_{50} ± SD (μM) (fold-reversal)			
	MCF-7		**MCF-7/adr (ABCB1)**	
Doxorubicin (μM)	0.081±0.010	(1.0)	14.263±1.423	(1.0)
+1.25 μM FG020326	0.085±0.014	(1.0)	2.219±0.222**	(6.4)
+2.5 μM FG020326	0.080±0.017	(1.0)	1.481±0.117**	(9.6)
+5 μM FG020326	0.089±0.021	(0.9)	0.996±0.134**	(14.3)
Vincristine (μM)	0.059±0.009	(1.0)	4.017±0.656	(1.0)
+1.25 μM FG020326	0.063±0.012	(0.9)	1.715±0.165**	(2.3)
+2.5 μM FG020326	0.057±0.014	(1.0)	0.874±0.287**	(4.6)
+5 μM FG020326	0.065±0.016	(0.9)	0.375±0.089**	(10.7)
Paclitaxel (nM)	6.905±0.903	(1.0)	339.772±38.655	(1.0)
+1.25 μM FG020326	5.847±1.212	(1.1)	98.274±16.325**	(3.5)
+2.5 μM FG020326	7.093±0.881	(1.0)	38.503±7.623**	(8.8)
+5 μM FG020326	7.133±0.651	(1.0)	15.453±3.588**	(22.0)
Cisplatin (μM)	3.553±0.213	(1.0)	2.650±0.252	(1.0)
+5 μM FG020326	3.250±0.305	(0.9)	2.941±0.325	(0.9)
	KB		KBv200 (ABCB1)	
Doxorubicin (μM)	0.020±0.010	(1.0)	0.979±0.123	(1.0)
+1.25 μM FG020326	0.019±0.012	(1.0)	0.234±0.028**	(4.2)
+2.5 μM FG020326	0.020±0.018	(1.0)	0.123±0.018**	(8.0)
+5 μM FG020326	0.022±0.020	(0.9)	0.080±0.024**	(12.2)
Vincristine (μM)	0.028±0.009	(1.0)	1.318±0.256	(1.0)
+1.25 μM FG020326	0.023±0.013	(1.0)	0.079±0.025**	(16.7)
+2.5 μM FG020326	0.024±0.012	(1.0)	0.038±0.011**	(34.7)
+5 μM FG020326	0.024±0.010	(1.0)	0.023±0.005**	(57.3)
Paclitaxel (nM)	1.383±0.148	(1.0)	48.342±4.119	(1.0)
+1.25 μM FG020326	1.333±0.162	(1.0)	9.583±1.039**	(5.0)
+2.5 μM FG020326	1.306±0.225	(1.0)	4.696±0.415**	(10.3)
+5 μM FG020326	1.387±0.130	(1.1)	1.590±0.116**	(30.4)
5-FU (μM)	3.561±0.379	(1.0)	3.122±0.324	(1.0)
+5 μM FG020326	3.431±0.358	(1.0)	3.302±0.210	(0.7)

	IC_{50} ± SD (μM) (fold-reversal)			
	MCF-7		**MCF-7/adr (ABCB1)**	
	KB-3-1		KB-CV60 (ABCC1)	
Vincristine (μM)	7.261±0.724	(1.0)	88.562±8.279	(1.0)
+5 μM FG020326	8.029±0.810	(0.9)	95.429±9.351	(0.9)
	NIH3T3		NIH3T3/MRP-4-2 (ABCC4)	
Vincristine (μM)	0.324±0.024	(1.0)	7.247±0.779	(1.0)
+5 μM FG020326	0.378±0.056	(0.9)	8.259±1.951	(0.9)
	S1		S1-M1-80 (ABCG2)	
Topotecan (μM)	0.084±0.024	(1.0)	12.031±1.279	(1.0)
+5 μM FG020326	0.192078±0.010	(1.1)	11.407±1.351	(1.0)
	SW1573		SW1573/2R120 (LRP)	
Doxorubicin (μM)	0.116±0.024	(1.0)	1.545±0.279	(1.0)
+5 μM FG020326	0.089±0.020	(1.2)	1.536±0.351	(1.0)

Cell survival was determined by MTT assay as described in “Materials and Methods”. Data are the means ± SD of at least three independent experiments performed in triplicate. The fold-reversal of MDR was calculated by dividing the IC_{50} for cells with the anticancer drug in the absence of FG020326 by that obtained in the presence of FG020326.

** represents $P<0.01$ for the values versus that obtained in the absence of FG020326.

Table 2

Effect of FG020326 on the reversal of MDR in KBv200 cell xenografts

Group	Pre-experiment		Post-experiment		Weight of	Growth
	n	Weight (g)	n	Weight (g)	tumor (g)	Inhibition (%)
Control	10	23.4±1.7	10	25.4±1.5	2.68±1.18	
FG020326	10	23.0±1.4	10	25.3±1.3	2.43±0.70	9.4
VCR	10	23.0±1.4	10	25.6±1.9	2.92±0.94	8.9
VCR+FG	10	23.6±1.3	10	25.4±1.6	1.25±0.23**	46.7
Control	10	21.7±3.2	10	26.6±3.2	2.24±1.11	
FG020326	10	22.1±1.7	10	27.0±2.7	2.08±1.00	7.2
Paclitaxel	10	20.8±2.6	10	24.4±2.6	2.06±1.06	8.1
Paclitaxel+FG	10	20.9±1.9	10	22.5±2.2	1.08±0.64**	51.7

The experiments were conducted as described in “Materials and Methods”. The values presented are the means ± SD for each group. FG: FG020326

** represents $P<0.01$ for the values versus that obtained in control group.

Table 3

Pharmacokinetic parameters of paclitaxel between vehicle- and FG020236-treated mice

Parameter	Without FG020326	With FG020326
$T_{1/2}\boldsymbol{\alpha}$ / h	0.55±0.04	0.48±0.04*
$T_{1/2}\boldsymbol{\beta}$ / h	1.53±0.06	1.42±0.08*
V_d/ml	12.39±1.10	10.91±1.59*
CL/ml·h^{-1}	5.33±0.53	5.64±0.59*
$AUC_{0\rightarrow 12/}$ h·ng·ml^{-1}	73560.64±5579.93	69437.66±2261.53*
$AUC_{0\rightarrow \infty /}$ h·ng·ml^{-1}	73683.7±5566.34	69715.33±2249.92*
MRT/h	1.54±0.02	1.6±0.05*

The main pharmacokinetic parameters of paclitaxel were summarized between two group mice pretreated with or without FG020326. The mice in experimental group were treated and plasma samples were assayed for paclitaxel as described in “Materials and Methods”. The paclitaxel plasma concentration-time data were analyzed using non-compartment model analysis to determine distribution half life ($t_{1/2}\alpha$), half life ($t_{1/2}\beta$), apparent volume of distribution (Vd), plasma clearance (CL), area under the curve (AUC) and mean retention time (MRT). The data represent the means and standard deviations of three independent samples.

* *P>0.05* for values *versus* those in paclitaxel alone.